

EVOLUTIONARY BIOLOGY

New skulls and skeletons of the Cretaceous legged snake *Najash*, and the evolution of the modern snake body plan

Fernando F. Garberoglio^{1*}, Sebastián Apesteguía¹, Tiago R. Simões^{2†}, Alessandro Palci^{3,4}, Raúl O. Gómez⁵, Randall L. Nydam⁶, Hans C. E. Larsson⁷, Michael S. Y. Lee^{3,4}, Michael W. Caldwell^{2,8}

Snakes represent one of the most dramatic examples of the evolutionary versatility of the vertebrate body plan, including body elongation, limb loss, and skull kinesis. However, understanding the earliest steps toward the acquisition of these remarkable adaptations is hampered by the very limited fossil record of early snakes. Here, we shed light on the acquisition of the snake body plan using micro-computed tomography scans of the first three-dimensionally preserved skulls of the legged snake *Najash* and a new phylogenetic hypothesis. These findings elucidate the initial sequence of bone loss that gave origin to the modern snake skull. Morphological and molecular analyses including the new cranial data provide robust support for an extensive basal radiation of early snakes with hindlimbs and pelves, demonstrating that this intermediate morphology was not merely a transient phase between limbed and limbless body plans.

INTRODUCTION

Snakes are a diverse and highly modified lineage of lizards with a long but sparse fossil record, beginning in the upper Middle Jurassic (1). Anatomical adaptations from their ancestral lizard-like skull condition include greatly increased gape size, increased skull kinesis, loss of temporal bones, and expansion of the attachment sites for the jaw adductor musculature. This highly modified skull creates difficulties in identifying homologies with other squamates, resulting in problems reconstructing phylogeny and in understanding the evolutionary acquisition and assembly of the snake skull and elongate body. Despite their limited fossil record, terrestrial and marine deposited sediments from Late Cretaceous Gondwana and its coastal regions preserve some of the oldest known articulated snake remains in the world (2–6). Here, we report eight new skulls and three articulated postcrania of the Cenomanian legged snake *Najash* (Patagonia, Argentina) (Figs. 1 and 2 and Supplementary Materials), previously known mainly from one articulated partial postcranial skeleton and a partial cranium and associated fragments (6–9). The new skull specimens include a new and near perfectly preserved three-dimensional skull that, by itself, clarifies several long-standing problems on the origin of key features of the modern snake skull. These new *Najash* specimens reveal a mosaic of primitive lizard-like features such as a large triradiate jugal and absence of the crista circumfenestralis, derived snake features such as the absence of the postorbital, as well as

intermediate conditions such as a vertically oriented quadrate. The new cranial data also robustly resolve the phylogenetic position of this crucial snake taxon, along with other limbed snakes.

The new three-dimensional, largely uncrushed fossils are found in rocks deposited in dune/interdune depositional environments (10) exposed in the La Buitrera Palaeontological Area (LBPA) (9). Material from this rare Lagerstätte makes *Najash* the best-known Mesozoic fossil snake taxon, followed closely by similar materials and ontogenetic stages of the slightly younger (Santonian-Campanian; Upper Cretaceous) but geographically proximate fossil snake *Dinilysia* (4, 11–14). Other key undisputed Mesozoic Gondwanan snakes include several terrestrial forms, all known only from single specimens: the Maastrichtian *Sanajeh* (15) and *Menarana* (16), and, most recently, the Cenomanian forest-dwelling snake *Xiaophis* (17), as well as marine forms represented by articulated specimens of limbed snakes from the Middle East, the Cenomanian simoliophiids *Pachyrhachis* (2), *Eupodophis* (3), and *Haasiophis* (5).

RESULTS

The new specimens exhibit a similar overall morphology that permits their assignment to the genus *Najash*; however, pending a full taxonomic review and assessment of the morphological diversity and disparity, the snakes from the LBPA are here conservatively assigned to *Najash* sp. (see the Supplementary Materials). MPCA 500 is preserved in three dimensions, with the right side in perfect articulation from the quadrate to the fragmentary premaxilla; the left side of the skull is broken away and lost, revealing internal and medial aspects of the right nasal, vomer, septomaxilla, and frontal; the parabasi-sphenoid rostrum; and the parietal (Figs. 1 and 2 and fig. S1).

For a detailed analysis of its skull anatomy, in addition to standard light microscopy studies, we performed high-resolution computed tomography (CT) scanning of the best-preserved skull (MPCA 500), revealing substantial new anatomical data on the early evolution of the snake skull (Fig. 2 and fig. S1). On the basis of morphology and topology (18), MPCA 500 unequivocally has a large jugal bone, similar to that found in many non-ophidian lizards and consistent with

Copyright © 2019
The Authors, some
rights reserved;
exclusive licensee
American Association
for the Advancement
of Science. No claim to
original U.S. Government
Works. Distributed
under a Creative
Commons Attribution
NonCommercial
License 4.0 (CC BY-NC).

¹CONICET, Área de Paleontología, Fundación de Historia Natural Félix de Azara, CEBBAD, Universidad Maimónides, Hidalgo 775, 1405 Buenos Aires, Argentina.

²Department of Biological Sciences, University of Alberta, Edmonton, Alberta T6G 2E9, Canada.

³College of Science and Engineering, Flinders University, Adelaide, SA 5042, Australia.

⁴Earth Sciences Section, South Australian Museum, North Terrace, Adelaide, SA 5000, Australia.

⁵CONICET, Departamento de Biodiversidad y Biología Experimental/Departamento de Ciencias Geológicas, Facultad de Ciencias Exactas y Naturales, Universidad de Buenos Aires, Ciudad Universitaria, 1428 Buenos Aires, Argentina.

⁶Arizona College of Osteopathic Medicine, Midwestern University, 19555 N. 59th Ave., Glendale, AZ 85383, USA.

⁷Redpath Museum, McGill University, 859 Sherbrooke Street W., Montreal, Quebec H3A 0C4, Canada.

⁸Department of Earth and Atmospheric Sciences, University of Alberta, Edmonton, Alberta T6G 2E9, Canada.

*Corresponding author. Email: fernando.garberoglio@fundacionazara.org.ar

†Present address: Department of Organismic and Evolutionary Biology, Museum of Comparative Zoology, Harvard University, Cambridge, MA 02138, USA.

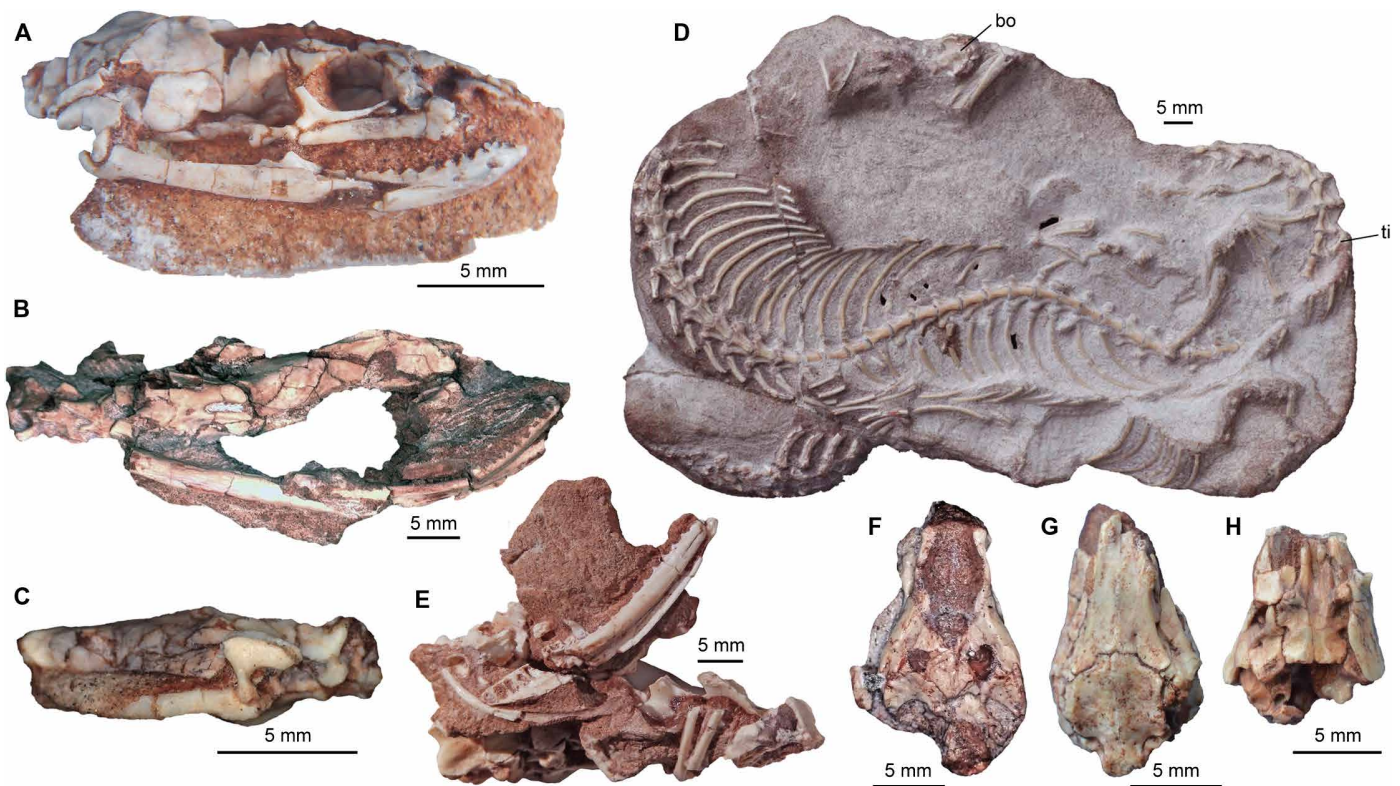


Fig. 1. *Najash* specimens from LBPA. (A) MPCA 500, skull with atlas-axis in right lateral view. **(B)** MPCA 591, partial skull with articulated vertebrae in right lateral view. **(C)** MPCA 581, partial skull with atlas in left lateral view. **(D)** MPCA 564, articulated specimen with partial skull and postcranium in ventral view. **(E)** MPCA 419, dentary and associated vertebrae and ribs. **(F)** MPCA 480, partial skull with atlas in dorsal view. **(G)** MPCA 536, partial skull in ventral view. **(H)** MPCA 386, partial skull in ventral view. bo, basioccipital; ti, tibia.

primary homologies proposed for other early fossil snakes such as *Pachyrhachis*, *Eupodophis*, *Yurlunggur*, and *Dinilyisia* (19). The unambiguous homology of the bone in MPCA 500 confirms the primary homology hypothesis in other fossil and modern snakes that this circumorbital bone is the jugal, not the postorbital. The jugal of *Najash*, like the triradiate element found in many lizards, has three major processes: an anterior ramus framing the ventrolateral margin of the orbit, superior to the maxilla, and contacting the prefrontal on the anteroventral orbital margin; a superior ramus framing the posterior margin of the orbit and contacting the posterior margin of the postfrontal and the parietal; and a short but robust posteroventral ramus contacting the ectopterygoid at the ectopterygoid-maxillary joint. This latter process presumably also served as a point of attachment for the quadratomaxillary ligament extending across the ventral margin of the lower temporal fenestra from the jugal-maxilla-ectopterygoid to the quadrate (19).

MPCA 500 and two more fragmentary skulls, MPCA 480 and MPCA 581, confirm that the quadrate in *Najash* was similar to that of *Dinilyisia* and some extant snakes, such as *Anilius*, in being oriented vertically rather than inclined anteroventrally or posteroventrally (Figs. 1 and 2 and fig. S1). Quadrate morphology is comparable to that of *Dinilyisia*, though on a smaller scale: The shaft is thin and narrow in lateral view but wide from the condyle to the large suprastapedial process in posterior view; the suprastapedial process is a large, gently curved process that is posteriorly elongate and dorsoventrally deep, providing a broad surface for articulation with the suprastapedial.

Nearly all extant snakes have a crista circumfenestralis, enclosing a unique bony chamber around the fenestra ovalis and lateral aperture of the recessus scalae tympani (20–22). The full crista circumfenestralis is composed of three cristae (tuberalis, interfenestralis, and prootica) that connect, or sometimes fuse, to form a chamber, the juxtastapedial recess, for an expanded perilymphatic sac that emerges from the recessus scalae tympani and surrounds the stapedia footplate (20). Arguments for a full crista circumfenestralis (6, 7, 12) versus incomplete, separate cristae (4, 9, 11, 20, 21) have been made in *Najash* and *Dinilyisia*. MPCA 500, and all other *Najash* cranial specimens preserving the otic capsular region of the otoocciput (Figs. 1 and 2 and fig. S1), indicates that a full crista circumfenestralis is absent but that at least two of the cristae are present: the crista interfenestralis, which separates the fenestra ovalis from the fenestra rotunda, and the crista tuberalis, which separates the vagus foramen from the fenestra rotunda (thus subdividing the original metotic fissure). However, a crista prootica is absent in *Najash*, as the stapedia footplate is not overlapped anteriorly by the prootic (Figs. 1 and 2 and fig. S1) (9, 21); the prootic forms a simple superior-anterior rim of the fenestra ovalis. In addition, the new materials refine previous observations made about the bony otic capsule, the footplate and columellar shaft of the stapes (and the inferred presence of an extra-columellar cartilage between the distal tip of the stapes and the quadrate suprastapedial process, similar to *Dinilyisia*, *Cylindrophis*, *Xenopeltis*, etc.), the fenestra ovalis and rotunda, and the metotic fissure and vagus foramen (see the Supplementary Materials). The stapedia footplate is large, covering a great proportion of the lateral

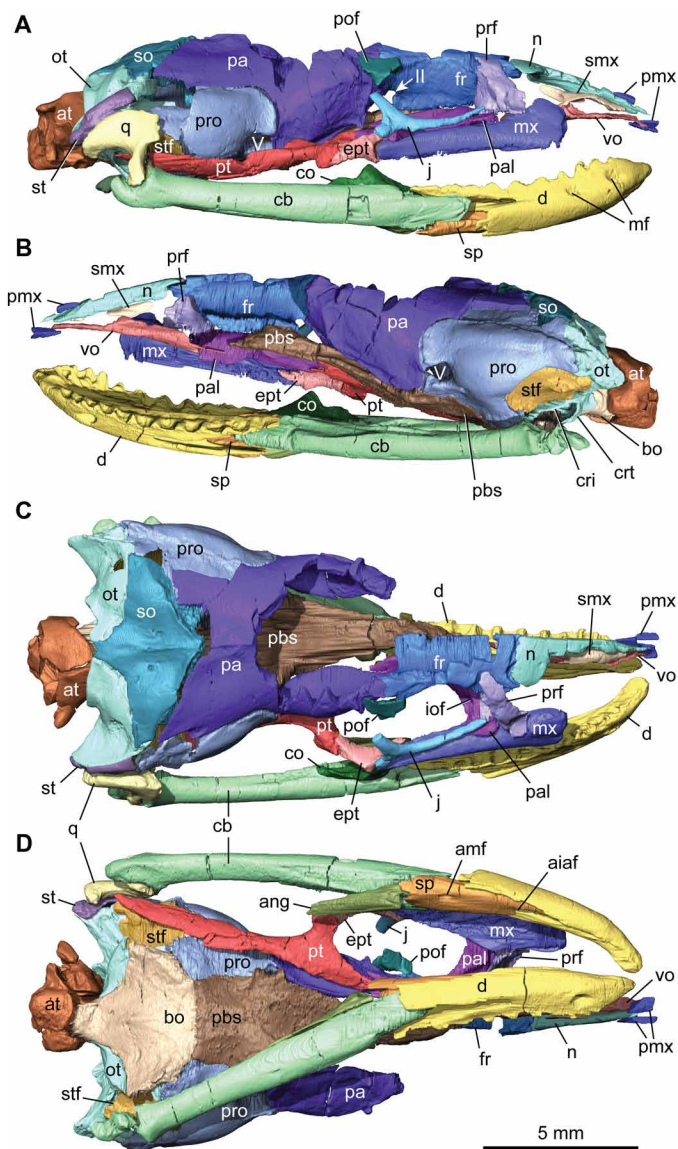


Fig. 2. CT scan reconstructions of the articulated skull of *Najash* (MPCA 500). (A) Right lateral view. (B) Left lateral view. (C) Dorsal view. (D) Ventral view. ll, optic foramen; V, trigeminal foramen; aiaf, anterior inferior alveolar foramen; amf, anterior or mylohyoid foramen; at, atlas-axis; ang, angular; bo, basioccipital; cb, compound bone; co, coronoid; cri, crista interfenestralis; crt, crista tuberalis; d, dentary; ept, ectopterygoid; fr, frontal; iof, infraorbital foramen; j, jugal; mf, mental foramina; mx, maxilla; n, nasal; ot, otoccipital; pa, parietal; pbs, parabasisphenoid; pal, palatine; pmx, premaxilla; pof, postfrontal; prf, prefrontal; pro, prootic; pt, pterygoid; q, quadrate; smx, septomaxilla; so, supraoccipital; sp, splenial; st, supratemporal; stf, stapedial footplate; vo, vomer.

surface of the bony otic capsule, a condition uniquely shared with *Dinilyisia* and “madtsoiids,” an extinct lineage of debated composition potentially including many taxa known only from vertebrae but usually restricted to the three better preserved taxa with skulls, *Sanajeh* (15), *Wonambi* (23), and *Yurlunggur* (24). The columellar shaft in all specimens is thick and robust relative to skull size, but because of the very small absolute size of most of the specimens, it is broken away near its contact with the quadrate suprastapedial process in all specimens; thus, this contact cannot be confirmed as

identical to that of *Dinilyisia* (fig. S1) (4). Last, there is no evidence of teeth on the palatine of MPCA 500 (fig. S1).

The phylogenetic relationships of Mesozoic snakes were analyzed using both Bayesian and parsimony methods on two separate datasets of fossil and modern snakes: a morphology-only dataset (1) and a combined morphological-molecular dataset (25). All analyses robustly recovered the Mesozoic Gondwanan forms *Najash*, *Dinilyisia*, and madtsoiids as basal snakes, outside modern (crown group) Serpentes. They form either a grade (Fig. 3 and figs. S2 and S3) or a clade (Fig. 4 and figs. S4 and S5) relative to modern snakes. The fossil vertebral form-taxon *Coniophis* emerges as either sister to or within crown Serpentes (Fig. 3 and fig. S5), contra a recent analysis (26) finding this taxon (both with or without putatively associated skull material) to be more basal. The affinities of the limbed Cretaceous marine snakes (simoliophiids) also emerge as basal snakes in most analyses (Figs. 3 and 4 and figs. S2 to S4). Notably, these basal positions for the terrestrial and marine limbed snakes are consistently retrieved, although relationships within crown snakes vary across the four analyses, mirroring current disagreements between different genomic datasets and between genomes and morphology. The placement of blind snakes (scolecophidians) varies most dramatically: Whereas morphological data alone provide support for a more derived position within extant snakes (Fig. 3 and fig. S2 and S3) than in most published morphological phylogenies [e.g., (1, 6–9, 12, 15, 26)], combined analysis, owing to the strong molecular signal, retrieves blind snakes as sister to all other extant snakes (Fig. 4 and fig. S4).

DISCUSSION

Assessing the phylogenetic position of *Najash* among other fossil and modern snakes has been difficult for several reasons: (i) numerous potential terminal taxa with highly variable anatomical features, (ii) strong previous disagreement on the identification of important anatomical components of fossil snakes (e.g., jugal versus postorbital and the nature of the crista circumfenestralis and its occurrence in early snake fossils) and its subsequent impact on the conceptualization and coding of morphological phylogenetic characters (27), (iii) strong disagreement between the morphological and the molecular signal for the placement of many extant taxa. We address these long-standing issues here, based on the numerous new specimens of *Najash*, and our reassessment of the known Mesozoic snake fossils with cranial material. These analyses clarify the evolutionary changes between lizards and the origin of modern (crown) snakes. It has also long been considered that a crista circumfenestralis was a necessary anatomical feature defining “snakeness” (7, 12, 28). However, the absence of the full crista circumfenestralis in *Najash* and other basal fossil snakes indicates that the crista circumfenestralis is not a diagnostic feature of all snakes but rather is a characteristic only of most, but not all, crown snakes and presents a highly variable morphology among those snakes. A reentrant fluid circuit may still have been present, though, in *Najash*, not fully bound by a bony crest system, similar to the condition in the few particular modern snakes lacking a full crista circumfenestralis (20, 28). Our analyses robustly support the basal phylogenetic position within snakes of the limbed terrestrial forms *Najash*, *Dinilyisia*, and madtsoiids and also suggest a similarly basal position for the limbed marine snakes (simoliophiids). The new cranial data [along with previously reported (7) and new postcranial data (9, 29)] retrieve this basal position even in the context of radical new molecular topologies for living snakes (Fig. 4 and fig. S4),

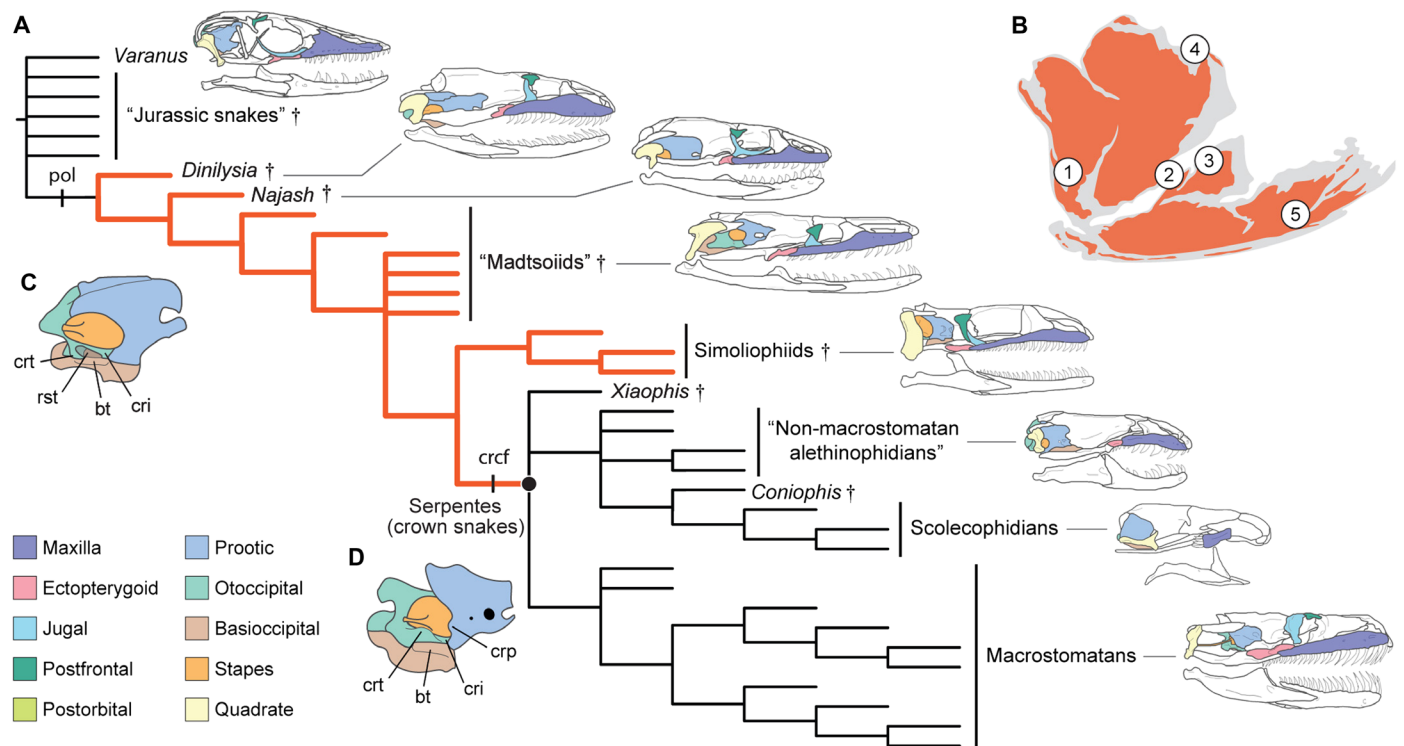


Fig. 3. Snake phylogeny and cranial evolution. (A) Majority-rule consensus of Bayesian inference analyses of dataset 1 (morphology-only). pol, postorbital loss; crcf, presence of full crista circumfenestralis (continuous system of bony crests surrounding the fenestra ovalis and the lateral aperture of the recessus scalae tympani, formed by prootic and otoccipital). Colored branch indicates Gondwanan radiation of basal snakes of Mesozoic origin as shown in the map (B) Gondwana during the Mesozoic, with the distribution of the fossil taxa in the analysis [1: *Najash* and *Dinilyisia* (Patagonia, Argentina); 2: *Menarana* (Madagascar); 3: *Sanajeh* (India); 4: simoliophiids (Middle East); 5: Cenozoic madtsoiids of Cretaceous origin (Australia)]; (C) otic region of *Najash*, showing the absence of crista circumfenestralis in basal snakes; and (D) otic region of *Anilius*, showing the presence of full crista circumfenestralis in Serpentes (crown or modern snakes) consisting of crista interfenestralis (cri), crista prootica (crp), and crista tuberalis (crt). bt, basal tubera; rst, lateral aperture of the recessus scalae tympani.

contrary to the most recent morphological and molecular analyses (30, 31). This basal position of the limbed terrestrial and marine snakes indicates that snakes retain sizeable external hindlimbs and sacral contacts for a substantial time after their origin—from approximately 170 Ma to the youngest confirmed legged snakes, the simoliophiids, at approximately 100 Ma. This indicates that (i) the reduction and loss of the pectoral girdle and forelimbs probably occurred much earlier, given the definitive absence of these structures in simoliophiids and the lack of evidence for their presence in *Najash*, *Dinilyisia*, and madtsoiids, and was probably a major event in the early radiation of snakes, and one that occurred well before crown (modern) snake origins; (ii) the “forelimb-absent and hindlimb-reduced” morphology was a stable and successful body plan, rather than a transient phase between limbed and limbless conditions; and (iii) the origin of crown snakes was characterized by a major reduction in the hindlimb and pelvis (including loss of sacral contacts). The identification of the posterior orbital element as the jugal (instead of the postorbital) demonstrates that the postorbital was lost very early in snake evolution (Fig. 3), probably at the same time as the loss of the upper temporal bar and likely some time before the loss of forelimbs, a condition common to other squamates (e.g., geckos, *Heloderma*, and *Lanthanotus*). *Najash* is now the best-known early snake and substantially clarifies the homologies of several problematic but key elements of the modern snake skull as well as the evolution of the skull from much more ancient snakes

and even earlier nonsnake lizards. These new materials of *Najash* shed light on the affinities of Late Mesozoic snakes and the successive evolutionary changes that led to the origin of modern snakes and one of the most remarkable vertebrate body plans.

MATERIALS AND METHODS

Materials

All the specimens of *Najash* come from the LBPA (9), a vast area in the Río Negro province (northern Patagonia, Argentina), northwest of the town of Cerro Policia, which includes within its extension a number of paleontological localities: La Buitrera, Cerro Policia, El Loro, La Escondida, and El Pueblito. The outcrops exposed at the LBPA belong to the upper section of the Candeleros Formation, the basal unit of the Neuquén Group, which is considered to have accumulated during the Cenomanian (32). These deposits underlie the Huincul Formation, dated by fission track analysis of a volcanic tuff unit at about 88 Ma (33). The snake specimens described here have been collected in three of these localities: La Buitrera Locality, Cerro Policia Locality, and El Pueblito Locality. Within each of these localities, snake remains were recovered from a large number of different sublocalities, sites, or one-off quarries (see list in the Supplementary Materials). In general, all the remains have been recovered as single, partially articulated specimens from a sandy succession that is considered to represent the interaction between fluvial and

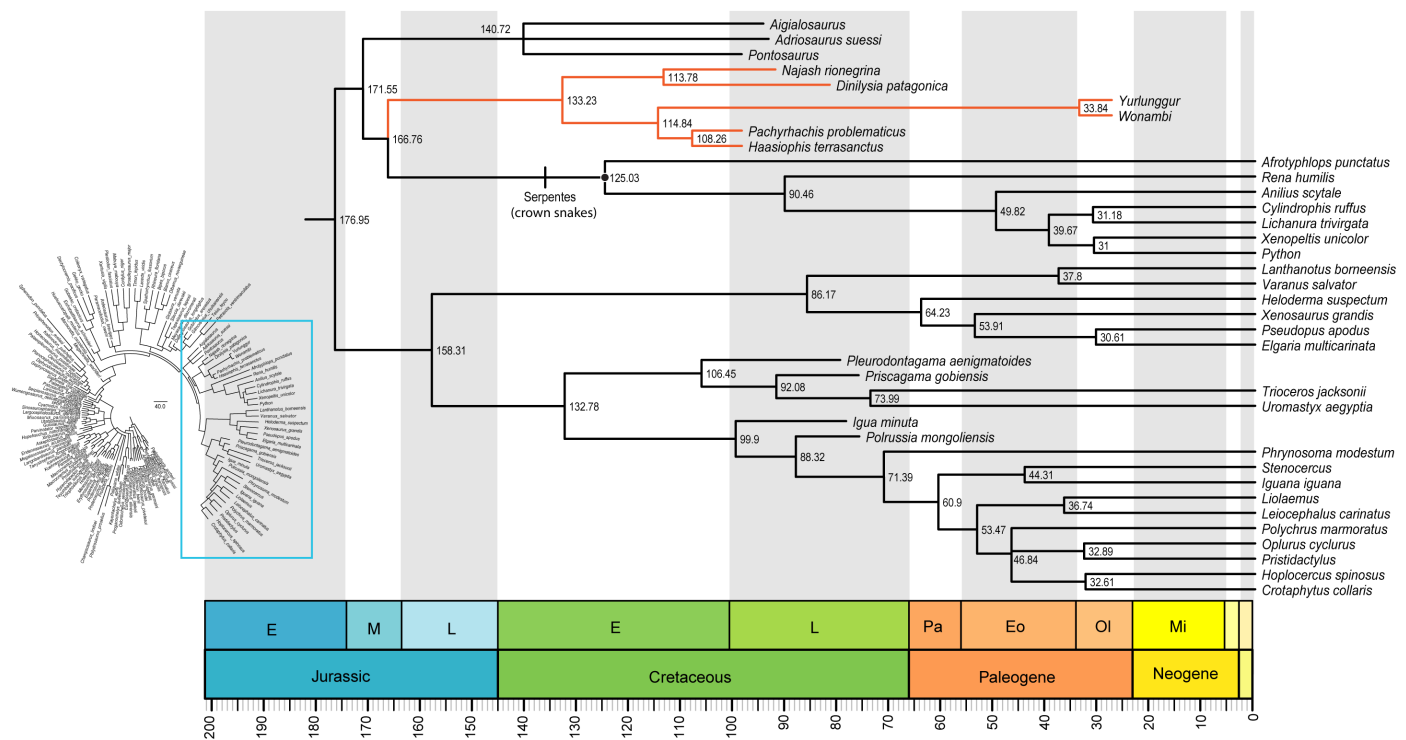


Fig. 4. Snake phylogeny and divergence times. Relaxed-clock Bayesian inference analysis of dataset 2 (combined evidence). Majority-rule consensus tree of the major diapsid and squamate lineages, with region of interest (blue square, see complete tree in fig. S4) zoomed in, showing snakes and closer clades against a geological time scale. Colored branch indicates Gondwanan radiation of basal snakes. Numbers at nodes indicate the median value for the divergence time estimates for each clade.

aeolian accumulations on the fringe of a large erg, the Kokorkom Desert (10). Most of the snake specimens have been collected from thick, cross-bedded sandstone beds that are related to the migration of relatively large aeolian dunes, often found associated with paleosols as evidenced by the presence of abundant rhizoliths and burrows.

Methods

X-ray CT

MPCA 500 was scanned at Universidad Maimónides. The scans were conducted with a spatial resolution of 7 to 8 μm .

Segmentation procedure

The skull of *Najash* (MPCA 500) was segmented in Avizo v.9.0 (Thermo Scientific). The stack of tiff images (1780 slices, 887 \times 930 pixels) was imported into the software, and the Threshold Tool was used to remove as much rock matrix as possible. However, in several parts of the specimen, the density of the bones approached that of the rock matrix, and several dense mineralizations and fractures prevented an effective removal of the rock matrix via thresholding without affecting the bones as well. Therefore, all the individual bones had to be manually segmented slice by slice, taking care of controlling the accuracy of the segmentation process via constant reference to the different views (three-dimensional and orthogonal views in the segmentation editor). The individual skull bones were segmented using the Lasso and Brush tools after locking the exterior and/or other already segmented bones. The segmented elements were then rendered as a surface (through the Generate Surface and Surface View modules) in Avizo v.9.0 and exported as stereolithography (stl) files.

Phylogenetic analyses

Two phylogenetic datasets were used to investigate the new data provided here: dataset 1, the snake phylogeny dataset of Caldwell *et al.* (1), with substantial modifications and expansions made by us (see the Supplementary Materials), and dataset 2, the recently published diapsid-squamate dataset of Simões *et al.* (25) to investigate the placement of snakes among other squamates and their divergence times based on morphological and molecular data (see also the Supplementary Materials).

Maximum parsimony analyses

Analyses were conducted in TNT 1.5-beta (34). For dataset 1, all heuristic searches were done under equal weights and consisted of 1000 rounds of random addition sequence of taxa followed by Tree Bisection Reconnection (TBR) branch swapping, holding 10 trees per replication, and collapsing branches of zero length after tree search. The resulting trees were subjected to a final round of TBR branch swapping, and optimal topologies were rooted with *Varanus*. A total of 392 most parsimonious trees (MPTs) were obtained with 624 steps each. The same analytical procedures were followed for the analysis of dataset 2 (morphological data only), and optimal topologies were rooted with *Protorothyris archeri*. A total of 432 MPTs were obtained with 2353 steps each.

Bayesian inference analyses

Analyses were conducted with MrBayes v.3.2.6 (35) using the Cedar computer cluster made available through Compute Canada and the CIPRES Science Gateway v.3.333. Molecular partitions were analyzed using the models of evolution obtained from PartitionFinder2 (36), and the morphological partition was analyzed with the Mk model (37) and a gamma distribution for the prior on rate variation among

characters [based on a previous assessment of the best-fitting model of rate variation for this dataset (25)].

Time-calibrated relaxed-clock Bayesian inference analyses

For dataset 2, we implemented “total-evidence-dating” using the fossilized birth-death tree model with sampled ancestors, under a relaxed-clock model in MrBayes v.3.2.6 (38), following the same procedures as in Simões *et al.* (25). The chosen relaxed-clock model is the independent gamma rate relaxed-clock model (39). The base of the clock rate was based on a preliminary nonclock analysis: the median value for tree height in substitutions from posterior trees divided by the age of the tree based on the median of the distribution for the root prior: $29.4493/325.45 = 0.09048$, in natural log scale = -2.402626 . Following Pyron (31), we chose to use the exponent of the mean to provide a broad standard deviation: $e^{0.09048} = 1.094699$. Sampling strategy was set to diversity, which is more appropriate when extant taxa are sampled in a way to maximize diversity (as performed here) and fossils are sampled randomly (38). The vast majority of our calibrations were based on tip-dating, which accounts for the uncertainty in the placement of fossil taxa and avoids the issue of bound estimates for node-based age calibrations (38). The fossil ages used for tip-dating correspond to the uniform prior distributions on the age range of the stratigraphic occurrence of the fossils (available in table S3). However, using tip-dates only can contribute to unrealistically older divergence time estimates for some clades (40). Therefore, for the clades for which we lacked some of the oldest known fossils in our analysis, for which there is overwhelming support in the literature (and in all our other analyses) regarding their monophyly, and for which the age of the oldest known fossil is well established, we used node age calibrations with a soft lower bound. Namely, these were captorhinids, choristoderes, snakes, and rhychocephalians [for more details, see the Supplementary Materials and also (27)]. Combined with diversity sampling strategy, the latter dating protocol can ensure reliable divergence time estimates. The age of the root was set with a soft lower bound to the same age as in Simões *et al.* (25). Convergence of independent runs was assessed using average standard deviation of split frequencies (ASDSF ~ 0.01), potential scale reduction factors (PSRF ≈ 1 for all parameters), and effective sample size (ESS) for each parameter greater than 200.

SUPPLEMENTARY MATERIALS

Supplementary material for this article is available at <http://advances.sciencemag.org/cgi/content/full/5/11/eaax5833/DC1>

Supplementary Text

Fig. S1. CT scan reconstructions disarticulating individual cranial elements of *Najash* (MPCA 500).

Fig. S2. Morphological data-only Bayesian inference analysis of dataset 2.

Fig. S3. Morphological data-only maximum parsimony analysis of dataset 2.

Fig. S4. Combined evidence relaxed-clock Bayesian inference analysis of dataset 2.

Fig. S5. Maximum parsimony analysis of dataset 1.

Fig. S6. Bayesian analysis of dataset 1.

Table S1. Measurements (length in millimeters) of the preserved portion of the selected elements of the described specimens.

Table S2. Stratigraphy and age for the newly included fossil taxa used for tip-dating calibrations.

Table S3. Accession numbers for the sampled molecular data for the additional extant taxa included here relative to the molecular data available in Simões *et al.* (25).

Movie S1. Micro-CT scan video of *Najash* skull MPCA 500, pitch mode.

Movie S2. Micro-CT scan video of *Najash* skull MPCA 500, roll mode.

Movie S3. Micro-CT scan video of *Najash* skull MPCA 500, yaw mode.

Data file S1. Nexus file for morphological phylogenetic ingroup dataset, with MrBayes command used for uncalibrated Bayesian analysis.

Data file S2. (Nexus_File_Dataset2_Combined_MrBayes) Nexus file for combined phylogenetic diapsid-squamate dataset with MrBayes command used for uncalibrated Bayesian analysis.

Data file S3. (Nexus_File_Dataset2_Combined_MrBayes_Clock) Nexus file for combined phylogenetic diapsid-squamate dataset with MrBayes command used for relaxed-clock Bayesian analysis.

Data file S4. (Nexus_File_Dataset2_MorphologyOnly) Nexus file for morphological phylogenetic diapsid-squamate dataset.

References (41–71)

[View/request a protocol for this paper from Bio-protocol.](#)

REFERENCES AND NOTES

- M. W. Caldwell, R. L. Nydam, A. Palci, S. Apesteguía, The oldest known snakes from the Middle Jurassic-Lower Cretaceous provide insight on snake evolution. *Nat. Commun.* **6**, 5996 (2015).
- M. W. Caldwell, M. S. Y. Lee, A snake with legs from the marine Cretaceous of the Middle East. *Nature* **386**, 705–709 (1997).
- J.-C. Rage, F. Escuillié, Un nouveau serpent bipède du Cénomanién (Cretacé). Implications phylétiques. *C. R. Acad. Sci. Paris Earth Sci.* **330**, 513–520 (2000).
- M. W. Caldwell, A. M. Albino, Exceptionally preserved skeletons of the Cretaceous *Dinilysia patagonica* Woodward, 1901. *J. Vertebr. Paleontol.* **22**, 861–866 (2003).
- O. Rieppel, H. Zaher, E. Tchernov, M. J. Polcyn, The anatomy and relationships of *Haasiophis terrasanctus*, a fossil snake with well-developed hind limbs from the mid-Cretaceous of the Middle East. *J. Paleontol.* **77**, 536–558 (2003).
- S. Apesteguía, H. Zaher, Cretaceous terrestrial snake with robust hindlimbs and a sacrum. *Nature* **440**, 1037–1040 (2006).
- H. Zaher, S. Apesteguía, C. A. Scanferla, The anatomy of the Upper Cretaceous snake *Najash rionegrina* Apesteguía and Zaher, 2006, and the evolution of limblessness in snakes. *Zool. J. Linnean Soc.* **156**, 801–826 (2009).
- A. Palci, M. W. Caldwell, A. M. Albino, Emended diagnosis and phylogenetic relationships of the upper Cretaceous fossil snake *Najash rionegrina* Apesteguía and Zaher, 2006. *J. Vertebr. Paleontol.* **33**, 131–140 (2013).
- F. F. Garberoglio, R. O. Gómez, S. Apesteguía, M. W. Caldwell, M. L. Sánchez, G. Veiga, A new specimen with skull and vertebrae of *Najash rionegrina* (Lepidosauria: Ophidia) from the early Late Cretaceous of Patagonia. *J. Syst. Palaeontol.* **17**, 1533–1550 (2019).
- D. J. Candia Halupczok, M. L. Sánchez, G. D. Veiga, S. Apesteguía, Dinosaur tracks in the Kokorkom Desert, Candeleros Formation (Cenomanian, Upper Cretaceous), Patagonia Argentina: Implications for deformation structures in dune fields. *Cretac. Res.* **83**, 194–206 (2017).
- R. Estes, T. H. Frazzetta, E. E. Williams, Studies on the fossil snake *Dinilysia patagonica* Smith Woodward: Part I. Cranial morphology. *Bull. Mus. Comp. Zool.* **140**, 25–74 (1970).
- H. Zaher, C. A. Scanferla, The skull of the Upper Cretaceous snake *Dinilysia patagonica* Smith-Woodward, 1901, and its phylogenetic position revisited. *Zool. J. Linnean Soc.* **164**, 194–238 (2012).
- C. A. Scanferla, B. A. S. Bhullar, Postnatal development of the skull of *Dinilysia patagonica* (Squamata-Stem Serpentes). *Anat. Rec.* **297**, 560–573 (2014).
- L. N. Triviño, A. M. Albino, M. T. Dozo, J. D. Williams, First natural endocranial cast of a fossil snake (Cretaceous of Patagonia, Argentina). *Anat. Rec.* **301**, 9–20 (2018).
- J. A. Wilson, D. M. Mohabey, S. E. Peters, J. J. Head, Predation upon hatchling dinosaurs by a new snake from the Late Cretaceous of India. *PLOS Biol.* **8**, e1000322 (2010).
- T. C. Laduke, D. W. Krause, J. D. Scanlon, N. J. Kley, A Late Cretaceous (Maastrichtian) snake assemblage from the Maevarano Formation, Mahajanga Basin, Madagascar. *J. Vertebr. Paleontol.* **30**, 109–138 (2010).
- L. Xing, M. W. Caldwell, R. Chen, R. L. Nydam, A. Palci, T. R. Simões, R. C. McKellar, M. S. Y. Lee, Y. Liu, H. Shi, K. Wang, M. Bai, A mid-Cretaceous embryonic-to-neonate snake in amber from Myanmar. *Sci. Adv.* **4**, eaat5042 (2018).
- C. Patterson, Morphological characters and homology, in *Problems of Phylogenetic Reconstruction*, K. A. Joysey, A. E. Friday, Eds. (Academic Press, 1982), pp 21–74.
- A. Palci, M. W. Caldwell, Primary homologies of the circumorbital bones of snakes. *J. Morphol.* **274**, 973–986 (2013).
- A. Palci, M. W. Caldwell, The Upper Cretaceous snake *Dinilysia patagonica* Smith-Woodward, 1901, and the Crista Circumfenestralis of snakes. *J. Morphol.* **275**, 1187–1200 (2014).
- M. W. Caldwell, J. Calvo, Details of a new skull and articulated cervical column of *Dinilysia patagonica* Woodward, 1901. *J. Vertebr. Paleontol.* **28**, 349–362 (2008).
- I. L. Baird, A survey of the periotic labyrinth in some representative recent reptiles. *Univ. Kans. Sci. Bull.* **41**, 891–981 (1960).
- J. D. Scanlon, Cranial morphology of the Plio-Pleistocene giant madtsoiid snake *Wonambi naracoortensis*. *Acta Paleontol. Pol.* **50**, 139–180 (2005).
- J. D. Scanlon, Skull of the large non-macrostromatan snake *Yurlunggur* from the Australian Oligo-Miocene. *Nature* **439**, 839–842 (2006).
- T. R. Simões, M. W. Caldwell, M. Talanda, M. Bernardi, A. Palci, O. Vernygora, F. Bernardini, L. Mancini, R. L. Nydam, The origin of squamates revealed by a Middle Triassic lizard from the Italian Alps. *Nature* **557**, 706–709 (2018).

26. N. R. Longrich, B.-A. S. Bhullar, J. A. Gauthier, A transitional snake from the Late Cretaceous period of North America. *Nature* **488**, 205–208 (2012).
27. T. R. Simões, M. W. Caldwell, A. Palci, R. L. Nydam, Giant taxon-character matrices: Quality of character constructions remains critical regardless of size. *Cladistics* **33**, 198–219 (2017).
28. O. Rieppel, H. Zaher, The development of the skull in *Acrochordus granulatus* (Schneider) (Reptilia: Serpentes), with special consideration of the otico-occipital complex. *J. Morphol.* **249**, 252–266 (2001).
29. F. F. Garberoglio, R. O. Gómez, T. R. Simões, M. W. Caldwell, S. Apesteguiá, The evolution of the axial skeleton intercentrum system in snakes revealed by new data from the Cretaceous snakes *Dinilysia* and *Najash*. *Sci. Rep.* **9**, 1276 (2019).
30. T. W. Reeder, T. M. Townsend, D. G. Mulcahy, B. P. Noonan, P. L. Wood Jr., J. W. Sites Jr., J. J. Wiens, Integrated analyses resolve conflicts over squamate reptile phylogeny and reveal unexpected placement for fossil taxa. *PLOS ONE* **10**, e0118199 (2015).
31. A. R. Pyron, Novel approaches for phylogenetic inference from morphological data and total-evidence dating in squamate reptiles (lizards, snakes, and amphisbaenians). *Syst. Biol.* **66**, 38–56 (2017).
32. H. A. Leanza, S. Apesteguiá, F. E. Novas, M. S. de la Fuente, Cretaceous terrestrial beds from the Neuquén Basin (Argentina) and their tetrapod assemblages. *Cretac. Res.* **25**, 61–87 (2004).
33. H. Corbella, F. E. Novas, S. Apesteguiá, H. A. Leanza, First fission-track age for the dinosaur-bearing Neuquén Group (Upper Cretaceous), Neuquén Basin, Argentina. *Rev. Mus. Argent. Cienc. Nat.* **6**, 227–232 (2004).
34. P. A. Goloboff, J. S. Farris, K. C. Nixon, TNT, a free program for phylogenetic analysis. *Cladistics* **24**, 774–786 (2008).
35. F. Ronquist, M. Teslenko, P. van der Mark, D. L. Ayres, A. Darling, S. Höhna, B. Larget, L. Liu, M. A. Suchard, J. P. Huelsenbeck, MrBayes 3.2: Efficient Bayesian phylogenetic inference and model choice across a large model space. *Syst. Biol.* **61**, 539–542 (2012).
36. R. Lanfear, P. B. Frandsen, A. M. Wright, T. Senfeld, B. Calcott, PartitionFinder 2: New methods for selecting partitioned models of evolution for molecular and morphological phylogenetic analyses. *Mol. Biol. Evol.* **10**, 772–773 (2017).
37. P. O. Lewis, A likelihood approach to estimating phylogeny from discrete morphological character data. *Syst. Biol.* **50**, 913–925 (2001).
38. C. Zhang, T. Stadler, S. Klopstein, T. A. Heath, F. Ronquist, Total-evidence dating under the fossilized birth–death process. *Syst. Biol.* **65**, 228–249 (2016).
39. T. Lepage, D. Bryant, H. Philippe, N. A. Lartillot, A general comparison of relaxed molecular clock models. *Mol. Biol. Evol.* **24**, 2669–2680 (2007).
40. J. E. O'Reilly, P. C. J. Donoghue, Tips and nodes are complementary not competing approaches to the calibration of molecular clocks. *Biol. Lett.* **12**, 20150975 (2016).
41. M. S. Y. Lee, J. D. Scanlon, Snake phylogeny based on osteology, soft anatomy and ecology. *Biol. Rev.* **77**, 333–401 (2002).
42. H. Zaher, J. A. Wilson, D. A. Mohabey, A new specimen of the nest predator *Sanajeh indicus* (Serpentes) suggests a more basal position within snake phylogeny, presented at the 77th Annual Meeting of the Society of Vertebrate Paleontology, Calgary, Canada, 25 August 2017.
43. J. C. List, Comparative osteology of the snake families Typhlopidae and Leptotyphlopidae. *Ill. Biol. Monogr.* **36**, 1–112 (1966).
44. A. Palci, M. W. Caldwell, R. L. Nydam, Reevaluation of the anatomy of the Cenomanian (Upper Cretaceous) hind-limbed marine fossil snakes *Pachyrhachis*, *Eupodophis*, and *Haasiophis*. *J. Vertebr. Paleontol.* **33**, 1328–1342 (2013).
45. M. W. Caldwell, R. R. Reisz, R. L. Nydam, A. Palci, T. R. Simões, *Tetrapodophis amplexus* (Crato Formation, Lower Cretaceous, Brazil) is not a snake, presented at the 76th Annual Meeting of the Society of Vertebrate Paleontology, Salt Lake City, UT, 26 October 2016.
46. M. S. Y. Lee, A. Palci, M. E. H. Jones, M. W. Caldwell, J. D. Holmes, R. R. Reisz, Aquatic adaptations in the four limbs of the snake-like reptile *Tetrapodophis* from the Lower Cretaceous of Brazil. *Cretac. Res.* **66**, 194–199 (2016).
47. J. D. Scanlon, *Nanowana* gen. nov., small Madtsoiid snakes from the Miocene of Riversleigh: Sympatric species with divergently specialised dentition. *Mem. Queensl. Museum* **41**, 393–412 (1997).
48. J.-C. Rage, Fossil snakes from the Paleocene of São José de Itaboraí, Brazil. Part I. Madtsoiidae, Aniliidae. *Palaeovertebrata* **27**, 109–144 (1998).
49. R. Hoffstetter, Un dentaire de *Madtsoia* (serpent géant du Paleocene de Patagonie). *Bull. Mus. Natl. Hist. Nat.* **31**, 379–386 (1959).
50. D. Cundall, F. Irish, The snake skull, in *Biology of the Reptilia*, C. Gans, A. S. Gaunt, K. Adler, Eds. (Oxford Univ. Press, 2008), vol. 20, pp 349–692.
51. O. Rieppel, N. Kley, J. A. Maisano, Morphology of the skull of the white-nosed blindsnake, *Liotyphlops albirostris* (Scoleophidia: Anomalepididae). *J. Morphol.* **270**, 536–557 (2009).
52. R. R. Pinto, A. R. Martins, F. Curcio, L. d. O. Ramos, Osteology and cartilaginous elements of *Trilepida salgueiroi* (Amaral, 1954) (Scoleophidia: Leptotyphlopidae). *Anat. Rec.* **298**, 1722–1747 (2015).
53. D. Cundall, D. A. Rossman, Cephalic anatomy of the rare Indonesian snake *Anomochilus weberi*. *Zool. J. Linn. Soc.* **109**, 235–273 (1993).
54. O. Rieppel, J. A. Maisano, The skull of the rare Malaysian snake *Anomochilus leonardi* Smith, based on high-resolution X-ray computed tomography. *Zool. J. Linn. Soc.* **149**, 671–685 (2007).
55. O. Rieppel, H. Zaher, The skull of the Uropeltinae (Reptilia, Serpentes), with special reference to the otico-occipital region. *Bull. Nat. Hist. Mus.* **68**, 123–130 (2002).
56. R. S. Comaux, J. C. Olori, C. J. Bell, Cranial osteology and preliminary phylogenetic assessment of *Plectrurus aureus* Beddome, 1880 (Squamata: Serpentes: Uropeltidae). *Zool. J. Linn. Soc.* **160**, 118–138 (2010).
57. J. C. Olori, C. J. Bell, Comparative skull morphology of uropeltid snakes (Alethinophidia: Uropeltidae) with special reference to disarticulated elements and variation. *PLOS ONE* **7**, e32450 (2012).
58. K. Katoh, D. M. Standley, MAFFT multiple sequence alignment software version 7: Improvements in performance and usability. *Mol. Biol. Evol.* **30**, 772–780 (2013).
59. J. G. Ogg, G. Ogg, F. M. Gradstein, *A Concise Geologic Time Scale* (Elsevier, 2016).
60. M. E. H. Jones, C. L. Anderson, C. A. Hipsley, J. Müller, S. E. Evans, R. R. Schoch, Integration of molecules and new fossils supports a Triassic origin for Lepidosauria (lizards, snakes, and tuatara). *BMC Evol. Biol.* **13**, 208 (2013).
61. S. E. Evans, New material of *Ctenogenys* (Reptilia: Diapsida; Jurassic) and a reassessment of the phylogenetic position of the genus. *Neues Jahrb. Geol. Paläontol.* **1989**, 577–589 (1989).
62. R. R. Schoch, D. Seegis, A Middle Triassic palaeontological gold mine: The vertebrate deposits of Vellberg (Germany). *Palaeogeogr. Palaeoclimatol. Palaeoecol.* **459**, 249–267 (2016).
63. R. R. Schoch, H.-D. Sues, Osteology of the Middle Triassic stem-turtle *Pappochelys rosinae* and the early evolution of the turtle skeleton. *J. Syst. Palaeontol.* **16**, 927–965 (2017).
64. J. Müller, R. R. Reisz, An Early Captorhinid Reptile (Amniota, Eureptilia) from the Upper Carboniferous of Hamilton, Kansas. *J. Vertebr. Paleontol.* **25**, 561–568 (2005).
65. M. J. Benton, P. C. Donoghue, R. J. Asher, M. Friedman, T. J. Near, J. Vinther, Constraints on the time scale of animal evolutionary history. *Palaeontol. Electron.* **18**, 1–106 (2015).
66. O. Rieppel, The naso-frontal joint in snakes as revealed by high-resolution X-ray computed tomography of intact and complete skulls. *Zool. Anz.* **246**, 177–191 (2007).
67. A. Palci, M. S. Y. Lee, M. N. Hutchinson, Patterns of postnatal ontogeny on the skull and lower jaw of snakes as revealed by micro-CT scan data and three-dimensional geometric morphometrics. *J. Anat.* **229**, 723–754 (2016).
68. S. Vasile, Z. Csiki-Sava, M. Venczel, A new madtsoiid snake from the Upper Cretaceous of the Hateg Basin, Western Romania. *J. Vertebr. Paleontol.* **33**, 1100–1119 (2013).
69. J. D. Scanlon, M. S. Y. Lee, The Pleistocene serpent *Wonambi* and the early evolution of snakes. *Nature* **403**, 416–420 (2000).
70. A. Palci, M. W. Caldwell, J. D. Scanlon, First report of a pelvic girdle in the fossil snake *Wonambi naracoortensis* Smith, and a revised diagnosis for the genus. *J. Vertebr. Paleontol.* **34**, 965–969 (2014).
71. E. Tchernov, O. Rieppel, H. Zaher, M. J. Polcyn, L. L. Jacobs, A fossil snake with limbs. *Science* **287**, 2010–2012 (2000).

Acknowledgments: We thank the Secretaría de Cultura de Río Negro for granting fieldwork permits in Río Negro Province. We thank the Pincheira, Mariluan, and Avelás families for allowing access to the study area. For fieldwork assistance, we thank G. W. Rougier, L. Triviño, L. Gaetano, R. Vera, G. Turazzini, E. Cimorelli, L. Fernández, and D. Mongue. For technical assistance, we thank A. Lindoe, L. J. Pazo, J. Kaluza, and R. Tahara. We would also like to thank two anonymous reviewers who certainly improved the manuscript. **Funding:** This work was supported by the CONICET scholarship (to F.F.G.); FONCyT-Agencia Nacional de Promoción Científica y Tecnológica, PICT N°2010-0564, and National Geographic grants 8826-10 and 9300-13 (to S.A.); an NSERC Discovery Grant (no. 234538) and Chairs Research Allowance (to M.W.C.); and Australian Research Council (ARC) grant DP160103005 (to M.S.Y.L. and A.P.). Aspects of this research were supported by the CT Scanning Laboratory, Universidad Maimonides, Buenos Aires, and by micro-CT data analysis infrastructure and software provided by the Integrated Quantitative Biology Initiative, Canadian Foundation of Innovation project 33122 (to H.C.E.L.), and from infrastructure and software provided by M.S.Y.L. **Author contributions:** F.F.G., S.A., and M.W.C. conceived the project. S.A. led fieldwork and primary data collection, involving F.F.G., R.O.G., and M.W.C. F.F.G. and M.W.C. wrote the manuscript and supplementary information. F.F.G., S.A., M.W.C., T.R.S., H.C.E.L., R.O.G., and M.S.Y.L. contributed to the analytical work (CT scanning and phylogenetic analyses). A.P. carried out the segmentation work and created the three-dimensional renderings. F.F.G., R.O.G., and T.R.S.

edited the figures. All authors contributed to discussions and editing of the manuscript and supplementary information. **Competing interests:** The authors declare that they have no competing interests. **Data and materials availability:** All data needed to evaluate the conclusions in the paper are present in the paper and/or the Supplementary Materials. All fossil materials are available for study (request for access to the collections manager at the Museo Provincial Carlos Ameghino, Cipolletti, Argentina). All secondary data/metadata (taxon-character matrix, CT scans) are available in the main text or the Supplementary Materials, or upon request to the corresponding author.

Submitted 4 April 2019
Accepted 25 September 2019
Published 20 November 2019
10.1126/sciadv.aax5833

Citation: F. F. Garberoglio, S. Apesteguía, T. R. Simões, A. Palci, R. O. Gómez, R. L. Nydam, H. C. E. Larsson, M. S. Y. Lee, M. W. Caldwell, New skulls and skeletons of the Cretaceous legged snake *Najash*, and the evolution of the modern snake body plan. *Sci. Adv.* **5**, eaax5833 (2019).